ISSN 0376-5156
Geophytology 54(2): 151–170
November 2024

Fresh water dinoflagellate cysts and other non-pollen palynomorphs (NPP) from the late Holocene sediments of Harvey Lake, New Brunswick, Canada

Arun Kumar

Carleton Climate and Environment Research Group (CCERG), Department of Earth Sciences, Carleton University, 1125 Colonel By Drive, Ottawa, Ontario K1S 5B6, Canada. E-mail: arunkumarlko@hotmail.com

Manuscript received: 08 July 2024
Accepted for publication: 01 August 2024

ABSTRACT

Kumar A. 2024. Fresh water dinoflagellate cysts and other non-pollen palynomorphs (NPP) from the late Holocene sediments of Harvey Lake, New Brunswick, Canada. Geophytology 54(2): 151–170.

This study is part of a palaeotempestology research project studying the late Holocene sediments from lakes in New Brunswick, Canada. Forty lake gyttja samples from core HV-CR in Harvey Lake, New Brunswick were studied. Three hundred palynomorphs excluding the fungal morphotypes were counted from each sample. Counts included gymnosperm and angiosperm pollen, bryophytic and pteridophytic spores, algal palynomorphs, dinoflagellate cysts and zoomorphs. Overall, gymnosperm and angiosperm pollen dominate the palynomorph assemblage (83.19%). Non-pollen palynomorphs (NPP) are only 16.81% of the assemblage that includes algal palynomorphs (4.27%), dinoflagellate cysts (7.6%), and zoomorphs (4.9%). Following cysts of freshwater dinoflagellates were identified: *Peridinium gatunense* Nygaard, *Peridinium limbatum* (Stokes) Lemmermann, *Peridinium volzii* Lemmermann, *Peridinium willei* Huitfeldt-Kaas, *Parvodinium inconspicuum* (Lemmermann) Carty, and *Fusiperidinium wisconsinense* (Eddy) McCarthy, Gu, Mertens & Carbonell-Moore. In addition, rare specimens of *Peridinium* sp. cf. *P. bipes* and a few unidentified dinoflagellate cyst types were also observed. Several algal morphotypes such as *Pediastrum*, Spirogyra zygospores, *Ovoidites* sp., *Botryococcu*s sp., and *Lecaniella* sp. (Spirogyra zygospore) were observed including few unidentified algal cell types. Several zoomorph morphotypes were observed as well. They are *Katora arabica* A. Kumar 2023, *Katora oblonga* A. Kumar 2023, *Palaeostomocystis fritilla* Roncaglia 2004, lorica of *Keratella* sp., rotifer lorica, chiromonid mandibles, cladoceran claw, *Bosmina longirostris* head capsule, *Daphnia pulex* (limb), and *Eurycercus lamellatus* (limb). Although fungal palynomorphs were not counted, several morphotypes were observed. They are: *Inapertisporites* Hammen 1954, *Palambages morulosa* O. Wetzel 1961, *Multicellites* Kalgutkar & Janson. 2000, *Dictyosporites* Félix 1894 emend. Kalgutkar & Janson. 2000, *Glomus* Tul. & C. Tul. 1845, *Diporisporites* Hammen 1954, *Hypoxylonites* Elsik 1990, *Fractisporonites* R.T. Clarke 1965, *Dicellaesporites* Elsik 1968, *Didymoporisporonites* Sheffy & Dilcher 1971, *Papulosporonites* Schmied. & G. Schwab 1964 and *Monoporisporites* Hammen 1954. This study extends the biogeographical distribution of freshwater dinoflagellate cysts to lakes in southern New Brunswick, Canada.

Keywords: Holocene palynology, lacustrine dinoflagellate cysts, non-pollen palynomorphs (NPP), zoomorphs, eastern Canadian lake, palaeoenvironments.

INTRODUCTION

Studies on non-pollen palynomorphs (NPP) have been widespread ranging from tropical to high latitudes, and from marine to continental environments covering the entire Phanerozoic Eon and even earlier (Battison & Brasier 2012). These microfossils are microscopic parts belonging to a variety of plants, algae, fungi, protists

and invertebrates, and to a lesser extent whole organism such as dinoflagellates and dinoflagellate cysts. Generally, NPP get destroyed by standard maceration techniques used in palynological studies. Historically, they have been ignored as well in favour of pollen and spores. NPP studies began in Europe following palynological examination of a variety of sediments from various freshwater environments (van Geel 1972, 1976, 1986, 2001). Since then, there have been several publications on freshwater NPP from different parts of the world, for example, Australia (Cook 2009), Canada (Warner 2009, McCarthy et al. 2011, 2017, 2018), India (Limaye et al. 2007, 2017), Venezuela (Montoya et al. 2010) and Africa (Gelorini et al. 2012). These publications list several references on freshwater NPP studies from different parts of the world.

The organic matter content of lacustrine sediments including the NPP provides significant information about palaeoenvironments, climate change, and anthropogenic activities on local and regional ecosystems. It originates from the benthic microorganisms, and from the remains of organisms formerly living in the lake and its watershed (Meyers & Ishiwatari 1995). A useful overview of common NPP in lacustrine ecosystems was published by McCarthy et al. (2021) which provided a quick guide to identifying common NPP using a dichotomous scheme along with photomicrographs of several genera and discussed their value as palaeolimnological and palaeohydrological indicators.

There are several late-Quaternary palynological studies of lakes in central and eastern Canada. Anderson (1985) compiled all pollen stratigraphic sites published till 1983. The primary objective of these studies was to understand late-Quaternary stratigraphy, vegetation and climate history including the glacial/interglacial phases. The chronological framework was provided by radiocarbon dates in these studies. A survey of pollen diagrams in Anderson's (1985) paper shows that there are no counts of any NPP, clearly indicating that NPP were ignored in all such studies. Similarly, late Quaternary pollen stratigraphy of the Ottawa Valley-Lake Ontario region has several pollen diagrams covering the Champlain Sea section, but none of them show any NPP counts (Anderson 1988). Although, there are many reports of occurrence of marine macrofossils from the Champlain Sea sediments, such as ostracodes (Cronin 1988), microfauna (Hunt & Rathburn 1988), invertebrates (Rodrigues 1988, Wassenaar et al. 1988), marine mammals (Harington 1988), and fossil fishes (McAllister et al. 1988) indicating presence of marine and brackish water NPP in these sections. However, they were ignored. Mott & Farley-Gill (1981) published two late Quaternary pollen diagrams from Pink Lake and Ramsey Lake in Gatineau Park, Quebec that included the Champlain Sea sediments. These diagrams do not show any counts of NPP. At present I am studying palynology of another two cores from the Pink Lake in the Gatineau Park and have observed presence of a large numbers of NPP that includes freshwater dinoflagellate cysts, algal cells, fungal palynomorphs, rhizopods and other zoomorphs.

The objective of the present study is to document, describe and illustrate all NPP in the late Holocene sediments of Harvey Lake, New Brunswick, discuss their biological affinity, and their numerical and proportional abundance. This study demonstrates the biogeographical distribution of various NPP specially the freshwater dinoflagellate cysts in Harvey Lake in New Brunswick, Atlantic Canada.

AN OVERVIEW OF STUDIES ON QUATERNARY FRESHWATER DINOFLAGELLATE CYSTS

Fossil dinoflagellates in the lacustrine sediments are resting cysts of freshwater dinoflagellates that are frequently observed in palynological slides. Their fossilization is due to their acid-resistant

(dinosporin) wall composition. In a comprehensive study on freshwater dinoflagellate cysts, Mertens et al. (2012) provided an overview of all described cysts and evaluated cyst-theca relationships and taxonomic identifications. According to them there are approximately 350 freshwater dinoflagellate species, among them only 84 resting cysts species have been described. Thay also reviewed taxonomy, phylogeny, ecology and palaeocology of recent freshwater dinoflagellate cysts, and suggested that shape, wall ornamentation, the archeopyle characteristics and color were important morphological characteristics at the generic level and above.

Dinoflagellate cysts were widely studied from the marine sediments and are known to have a widespread distribution and a long marine fossil record (Penaud et al. 2018). However, the first fossil freshwater dinoflagellate cysts were reported from the Oligocene Brandon Lignite of Vermont, USA (Traverse 1955). In a later study, Norris & McAndrews (1970) described dinoflagellate cyst types A, B, C and D from the postglacial muds in Glatsch Lake, Minnesota, USA and morphologically related them respectively to the following extant freshwater dinoflagellate taxa: *Peridinium limbatum, Peridinium wisconsinense, Peridinium willei* and *Peridinium bipes*. However, McCarthy et al. (2011) suggested that types C and D of Norris & McAndrews (1970) could be attributed to the modern cyst of *Peridinium willei*. Earlier, only morphological criteria were used to identify and describe freshwater dinoflagellate cysts to species level (Norris and McAndrews 1970), and it was not always possible to establish a cyst-theca relationship.

Later research on culturing and DNA sequencing confirmed the identity of thecate *Peridinium willei* with its cyst. McCarthy et al. (2011) successfully established cyst–theca relationship by germinating cysts of freshwater dinoflagellates from surface sediments of Severn Sound, southeastern Georgian Bay (Lake Huron, Laurentian Great Lakes of North America). The cyst-theca relationship of two cyst morphotypes assigned to *Peridinium wisconsinense* Eddy 1930 and *Peridinium willei* Huitfeldt-Kaas 1900 was established through germinations and single-cell LSU rDNA analysis on an excysted cell of *Peridinium willei*. Since there is limited knowledge of geographic distribution of freshwater dinoflagellate cysts, the present study is significant because it provides additional information about biogeographic distribution of freshwater dinoflagellate cysts in the North American lakes.

Mertens et al. (2012) mentioned several publications on Quaternary freshwater dinoflagellate cysts including Norris & McAndrews (1970). Additional references are, Miller et al. (1982) who recovered cysts of the freshwater dinoflagellates *Peridinium cinctum, Peridinium limbatum* and *Peridinium wisconsinense* from the marine Bedford Basin, Nova Scotia, Canada from the early Holocene sediments, indicating a lower sea level. Burden et al. (1986) described high cyst abundance for *Peridinium willei* and *Peridinium wisconsinense* in two lakes in Awenda Provincial Park, Ontario, Canada and related them with land clearing changes causing a nutrient influx. Zippi et al. (1990) recovered cysts of *Peridinium bipes, Peridinium limbatum, Peridinium willei and Peridinium wisconsinense* from surface sediments in 11 lakes of the Haliburton-Muskoka region, Ontario, Canada. Chu et al. (2008, 2009) reported cysts of *Parvodinium* sp. cf. *P. inconspicuum* (Lemmermann) Carty in a 1600-year core from Lake Xiaolongwan, northeastern China. Tardio et al. (2006, 2009) reported *Parvodinium umbonatum* cysts from the low alkalinity, high altitude Lake Nero di Cornisello, Italy. McCarthy et al. (2011) related changes between *Peridinium willei* and *Peridinium wisconsinense* cysts to changes in cultural eutrophication in Severn Sound, Lake Huron.

In a series of publications Francine McCarthy and her associates demonstrated occurrence of freshwater dinoflagellate cysts in Quaternary Lake sediments of Ontario (Canada) and Massachusetts (USA). They corelated the occurrence of these cysts to various environmental and ecological factors establishing their palaeoecological and biogeographical significance. Their publications are mentioned here as follows. Occurrences of *Peridinium wisconsinense* and *Peridinium willei* in surface sediments from Severn Sound, southeastern Georgian Bay (McCarthy et al. 2011), *Peridinium willei* and *Peridinium volzii* in Lake Simcoe, Ontario (Danesh et al. 2013), *Peridinium wisconsinense, Peridinium inconspicuum, Peridinium willei* and *Peridinium volzii* in the southeast Great Lakes region of Ontario, Canada (McCarthy & Kruger 2013), *Peridinium* sp. cf. *P. gatunense, Peridinium* sp. cf. *P. volzii Lemmerman, Peridinium willei* and *Peridinium wisconsinense* from Sluice Pond, Massachusetts, USA (Drljepan et al. 2014), *Peridinium wisconsinense* and *Peridinium willei/P. volzii* from Lake Simcoe, Ontario (Volik et al. 2016), *Parvodinium* [*Peridinium*] *inconspicuum* and *Peridinium volzii* from the Crawford Lake – A Canadian Holocene Lacustrine Konservat-Lagerstätte (Kruger & McCarthy 2016), *Peridinium* sp. cf. *P. gatunense, Peridinium limbatum, Peridinium* sp. cf. *P. volzii, Peridinium willei, Peridinium wisconsinense* from Sluice Pond, a meromictic lake in NE Massachusetts, USA (McCarthy et al. 2017), taxonomic transfer of the freshwater dinoflagellate *Peridinium wisconsinense* (*Dinophyceae*) to the family *Thoracosphaeraceae*, and description of *Fusiperidinium* McCarthy et al. 2018a), *Peridinium volzii*, *P. willei, Parvodinium inconspicuum* and *Peridinium wisconsinense* from the lakes of the Great Lakes region (McCarthy et al. 2018b).

According to Mertens et al. (2012) only a few freshwater cysts have fossilization potential, viz. *Parvodinium* sp., *Parvodinium umbonatum*, five species of *Peridinium* (*Peridinium bipes, Peridinium cinctum, Peridinium limbatum, Peridinium willei, Peridinium wisconsinense*) and *Gonyaulax clevei* Ostenfeld. They have been identified from Quaternary sediments.

Danesh et al. (2024) compared the distribution of recent freshwater dinoflagellate cysts from 32 boreal lakes in northwestern Ontario with varying physical and chemical characteristics and found that cysts of *Fusiperidinium wisconsinense, Parvodinium umbonatum,* and *Peridinium willei* were nearly ubiquitous. However, cysts of *Parvodinium inconspicuum, Peridinium limbatum,* and *Peridinium volzii* were abundant but present in a smaller number of lakes. They broadly clustered the assemblages into three groups. They are: 1. an assemblage (primarily *Peridinium* spp.) associated with relatively shallow, mesotrophic lakes; 2. an assemblage dominated by *Fusiperidinium wisconsinense* in mesotrophic lakes with intermediate depth and relatively high pH and alkalinity; and 3. an assemblage dominated by *P. umbonatum* in deeper oligotrophic lakes.

HARVEY LAKE AND ITS ENVIRONMENT

Harvey Lake (45°43'45"N, 67°00'25"W) is located just north of Harvey, a small village in the province of New Brunswick, Canada (Figure 1). The surface area of this lake is 7.2 km^2 and has a maximum depth of 11.8 m. There are two small inlet streams and one outlet stream in the lake (Patterson et al. 2022). The lake is situated in the temperate climate zone where regional altitude ranges between 152–304 m above the mean sea level; the region's mean annual temperature is 5° C and mean annual precipitation is 1016 mm. The region surrounding the lake is covered by two types of mixed forests, one is the sugar maple-yellow birch-white pine, and other is the spruce-fir-maple-birch (Anderson 1985).

There is no time constraint on the core HV-

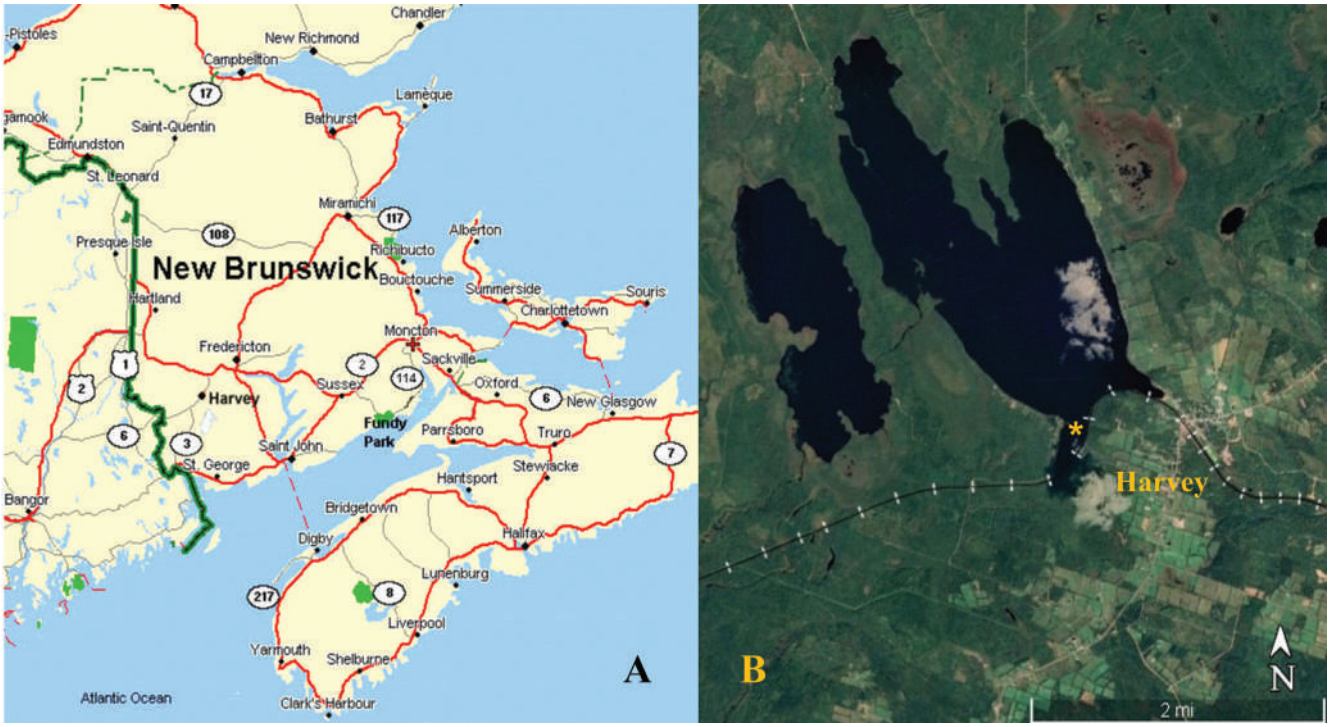

Figure 1 A: Map of a part of eastern Canada showing location of the Harvey village in the province of New Brunswick (source Wikipedia downloaded on June 26, 2024); **B**. Location of the core HV-CR collected in 2021 shown by a yellow Asterisk in the Harvey Lake, near Harvey, New Brunswick. (source Google Earth downloaded on June 26, 2024).

CR. However, radiocarbon dates for bulk samples from the two Harvey Lake Cores collected in 2017 are given in table 1 (Patterson et al. 2022) which shows that the age of the youngest sample in core HL-2017-GC-02 at depth 50–54 mm is Cal BP 660–620. Similarly, the oldest date is from the core HL-2017-GC-03 at depth 180–184 mm is Cal BP 6,728–6,556. The core HV-CR was collected in 2021 is in proximity of core HL-2017-GC-02. Thus, the dates provided in Patterson et al. (2022, Table 1) give an approximate idea about the time constraint of the core HV-CR.

MATERIAL AND METHODS

This study is based on 40 lake gyttja samples from the core HV-CR collected in 2021 (Figure 1B). The thickness of the core is approximately 40 cm, and two slides each from the 40 samples, about 10 mm apart, were prepared in 2023. One cubic cm of lake gyttja per sample was used in the maceration process, using standard palynological processing procedure and two slides per sample were prepared using the processing method described in Kumar (2020).

The slides were studied under an OMAX Optical Microscope (MD827S30L Series) using transmitted light. Each slide was scanned under ×400 magnification and palynomorphs were photographed at ×400 and ×1000 (oil immersion) using the microscope's built-in camera system. A few very large palynomorphs were photographed at ×100 as well. A total of 300 palynomorphs were counted from each sample excluding the fungal morphotypes. Dinoflagellate cysts were separately counted from algal remains. Algal remains include algal cells, unknown cysts, and algal filaments. Palynomorphs observed in this study are illustrated in figures 2, 3, 4 and 5. Table 1 shows the numerical distribution of palynomorphs including the NPP, and table 2 shows percentage distribution of NPP.

RESULTS

Generally, the samples yielded rich assemblages of well preserved and diverse groups of palynomorphs. However, samples 280–281 mm and 290–291 mm were barren. A total of 300 palynomorphs were counted from each sample, excluding the fungal palynomorphs (Table 1). The counts were divided into gymnosperm and angiosperm pollen; bryophytic and pteridophytic spores, algal palynomorphs, dinoflagellate cysts and zoomorphs. According to Traverse (1994) the zoomorphs are palynomorphs of metazoan affinity. The gymnospermous pollen include *Abies*, *Cupressaceae*, *Pinus, Picea and Tsuga* and angiospermous pollen include *Acer, Alnus,*

Table 1. Numerical distribution of pollen, spores and non-pollen palynomorphs.

Depth (in mm)	Gymnosperm	Angiosperm	Total Pollen	Spores	Algae	Dinocysts	Zoomorphs	Total NPP	Grand Total
2–3	183	53	236	5	9	25	25	59	300
9–10	182	58	240	10	15	16	19	50	300
20–21	161	54	215	14	20	26	25	71	300
30–31	177	61	238	13	11	21	17	49	300
40–41	151	84	235	7	16	30	12	58	300
51–52	160	69	229	3	19	31	18	68	300
62–63	182	79	261	9	3	22	5	30	300
70–71	137	111	248	21	7	17	7	31	300
80–81	147	76	223	5	18	35	19	72	300
90–91	130	97	227	13	19	31	10	60	300
101–102	153	80	233	13	12	26	16	54	300
110–111	181	58	239	11	11	17	22	50	300
120–121	159	62	221	20	15	29	15	59	300
130–131	143	81	224	17	12	31	16	59	300
140–141	163	54	217	13	18	34	18	70	300
151–152	160	66	226	19	15	27	13	55	300
160–161	203	35	238	11	14	21	16	51	300
170–171	157	69	226	15	12	30	17	59	300
180–181	168	54	222	26	9	25	18	52	300
190–191	170	51	221	19	8	31	21	60	300
201–202	164	71	235	16	9	25	15	49	300
210–211	174	68	242	15	12	21	10	43	300
220–221	160	58	218	12	23	23	24	70	300
230–231	173	57	230	13	16	26	15	57	300
240–241	166	67	233	15	19	21	12	52	300
251–252	159	80	239	24	6	12	19	37	300
260–261	214	28	242	9	7	24	18	49	300
270–271	184	56	240	11	9	23	17	49	300
280–281					Barran				
290–291					Barren				
301–302	151	78	229	23	12	25	11	48	300
310–311	148	86	234	22	14	21	9	44	300
320–321	181	42	223	13	18	29	17	64	300
330–331	150	92	242	12	15	21	10	46	300
340–341	174	77	251	15	10	17	7	34	300
351–352	122	114	236	19	13	20	12	45	300
360–361	174	82	256	9	11	16	8	35	300
370–371	165	82	247	14	11	15	13	39	300
380–381	169	84	253	19	8	13	7	28	300
390–391	181	81	262	8	12	11	7	30	300
Average	165.15	69.86	235.01	14.2	12.84	23.86	14.73	50.94	300

Ambrosia, Artemesia, Betula, Carpinus/Ostrya, *Poaceae*, *Populus, Quercus, Salix, Tilia*, *Ulmus* and few others. Table 2 shows percentage distribution of algal palynomorphs, dinoflagellate cysts and zoomorphs. Total percentage of NPP excluding the fungal palynomorphs is also given in Table 2.

Table 2. Percentage distribution of non-pollen palynomorphs.

Depth (in mm)	Algae %	Dinocysts %	Zoomorphs %	NPP %
2–3	3	8.33	8.33	19.66
9–10	5	5.33	6.33	16.66
20–21	6.66	8.66	8.33	23.65
30–31	3.66	7	5.66	16.32
40–41	5.33	10	4	19.33
51–52	6.33	10.33	6	22.66
62–63	1	7.33	1.66	9.99
70–71	2.33	5.66	2.33	10.32
80–81	6	11.66	6.33	23.99
90–91	6.33	10.33	3.33	19.99
101–102	4	8.66	5.33	17.99
110–111	3.66	5.66	7.33	16.65
120–121	5	9.66	5	19.66
130–131	4	10.33	5.33	19.66
140–141	6	11.33	6	23.33
151–152	5	9	4.33	18.33
160–161	4.66	7	5.33	16.99
170–171	4	10	5.66	19.66
180–181	3	8.33	6	17.33
190–191	2.66	10.22	7	19.88
201–202	3	8.33	5	16.33
210–211	4	7	3.33	14.33
220–221	7.66	7.66	8	23.32
230–231	5.33	8.66	5	18.99
240–241	6.33	3	4	13.33
251–252	2	4	6.33	12.33
260–261	2.33	8	6	16.33
270–271	3	7.66	5.66	16.32
280–281		Barran		
290–291		Barran		
301–302	4	8.33	3.66	15.99
310–311	4.66	7	3	14.66
320–321	6	9.66	5.66	21.32
330–331	5	7	3.33	15.33
340–341	3.33	5.66	2.33	11.32
351–352	4.33	6.66	4	14.99
360–361	3.66	5.33	2.66	11.65
370–371	3.66	3	4.33	10.99
380–381	2.66	4.33	2.33	9.32
390–391	4	3.66	2.33	9.99
Average	4.27	7.6	4.9	16.81

Gymnosperm pollen dominate the palynomorph assemblages, their average number in samples is 161.15 (53.66%). The average number of other palynomorphs is as follows: angiosperm pollen 69.86 (23.28%), total pollen 235.01 (78.33%), bryophytic and pteridophytic spores 14.2 (4.7%), algal palynomorphs 12.84 (4.28%), dinoflagellate cysts 23.86 (7.95%), zoomorphs 14.73 (4.91%), and total NPP 50.94 (16.98%). Percentage distribution of NPP is shown in table 2, where dinoflagellate cysts (7.6%) dominate the assemblage. Algal palynomorphs (4.27%) and zoomorphs (4.9%) are minor constituents and total NPP is 16.81%. This study concentrates primarily on freshwater dinoflagellate cysts. However, other NPP groups including the fungal palynomorphs were also recorded. But the fungal palynomorphs were not counted.

NON-POLLEN PALYNOMORPHS (NPP)

Several groups of non-pollen palynomorphs were observed in this study. They are documented and described below. Dinoflagellate cyst descriptions are primarily based on McCarthy et al. (2011) and Mertens et al. (2012). Generally, the resting cysts of freshwater dinoflagellates have relatively thick double walls, a smooth inner and an outer wall that usually bears ornamentation. Both the walls are usually closely appressed, for example, cysts of *Peridinium willei* and *Parvodinium inconspicuum* while others are distinctly cavate like *Fusiperidinium wisconsinense* (McCarthy et al. 2021).

1. Dinoflagellate cysts

The following freshwater dinoflagellate cysts were observed.

1.1. Cyst of *Peridinium gatunense* Nygaard (Figure 2.9–11): These are oval to round, proximocavate cysts, have smooth to finely granular walls, and granules in periphragm define a paracingulum. Extensions of the periphragm from the thick-walled endophragm produce

characteristic 'frills'(McCarthy et al. 2017). Mid-focus image shows the separation of the inner and outer wall in this proximocavate cyst (McCarthy et al. 2017). Size range (based on 6 specimens) 31–40 × 36–52 µm. Comments: Morphological description along with illustrations and previous occurrences of this species is discussed by Mertens et al. (2012).

1.2. Cyst of *Peridinium limbatum* (Stokes) Lemmermann (Figure 2.12, 13): These cysts are approximately pentagonal, cavate/proximate, have one short and blunt apical horn and two antapical horns. These morphotypes are relatively of larger size (92–104 µm long, 64–82 µm wide, Wall & Dale 1968). The inner wall is smooth, whereas the outer wall is covered by granules reflecting the paratabulation (McCarthy et al. 2017). Size range (based on two specimens) 51–53 × 44–50 µm. Comments: Present specimens are smaller than the size range reported by Wall & Dale (1968). Morphological description along with illustrations and previous occurrences of this species is discussed by Mertens et al. (2012).

1.3. Cysts of *Peridinium volzii* Lemmermann (Figure 2.14, 15): These cysts are oval, proximate, and cavate but the two layers are closely appressed, having a distinctive red body inside the cyst. The outer wall is relatively thin and finely textured, almost lacks ornamentation, and has less pronounced shoulders and lacks an apical flange thus morphologically differs from the cysts of *Peridinium willei* (McCarthy et al. 2013, 2017). Size range (based on five specimens) 39–44 × 32–36 µm. Comments: The cysts of *Peridinium volzii* are smaller than cysts of *Peridinium willei* (McCarthy et al. 2013, 2017). Mertens et al. (2012) state the following about *Peridinium volzii* **"**Described by Pfiester & Skvarla (1979) as having three walls: a thick exospore, a thin mesospore, and a thick endospore; from cultures established from a small pond in the Wichita Mountains, Commanche County (Oklahoma, U.S.A.)."

1.4. Cyst of *Peridinium willei* Huitfeldt-Kaas (Figure 2.5–8): These cysts are of round to sub-round or ellipsoidal shape, often dorso-ventrally compressed, cavate and proximate without horns. Both wall layers are closely appressed but also detached sometimes, inner wall is transparent and smooth. The outer wall is thick and smooth and is slightly invaginated in the sulcal area forming two distinct shoulders. The archeopyle type is usually not clearly discernible and appears to be formed by the loss of several angular plates in the apex indicating a transapical archeopyle (McCarthy et al. 2011, 2017). Earlier the archeopyle type in this morphotype was described as a transapical suture opening (Evitt & Wall 1968, Norris & McAndrews 1970). These cysts may have one or more yellowish and brownish red bodies within them. Size range (based on eight specimens) 33–40 × 39–51 µm. Comments: Morphological description along with illustrations and previous occurrences of this species is discussed by Mertens et al. (2012).

1.5. Cysts of *Parvodinium inconspicuum* (Lemmermann) Carty (Figure 2.16–17): These are very small ~15–22 µm, spherical

Figure 2. 1–4. Cyst of *Fusiperidinium wisconsinense* (Eddy) McCarthy et al. **1.** Slide 70–71 mm 1, 5.5 × 126.7, size 55 × 38 µm. **2.** Slide 101–102 mm 1, 6.5 × 128.5, size 53 × 38.7 µm. **3.** Slide 151–152 mm 1, 6 × 122.2, size 39 × 32 µm. **4.** Slide 201–202 mm 2, 4 × 125, size 51 × 41 µm. **5–8.** Cyst of *Peridinium willei* Huitfeldt-Kaas. **5.** Slide 330–331 mm 1, 16.8 × 137, size 51 × 41 µm. **6.** Slide 370–371 mm 1, 3.8 × 129.8, size 51 × 33 µm. **7.** Slide 340–341 mm 1, 6 × 133.8, size 44 × 34 µm. **8.** Slide 351–352 mm 1, 15 × 127.5, size 39 × 35 µm. **9–11.** Cyst of *Peridinium gatunense* Nygaard. **9.** Slide 201–202 mm 1, 12.5 × 134, size 46 × 40 µm. **10.** Slide 210–211 mm 1, 6.4 × 130.5, size 45 × 39 µm. **11.** Slide 360–361 mm 1, 12.5 × 127.3, size 44 × 40 µm. **12–13.** Cyst of *Peridinium limbatum* (Stokes) Lemmermann. **12.** Slide 340–341 mm 1, 8.3 × 135.5, size 49 × 36 µm. **13.** Slide 351–352 mm 1, 6.5 × 124.5, size 52 × 40 µm. **14–15.** Cyst of *Peridinium volzii* Lemmermann. **14.** Slide 390–391 mm 2, 15.5 × 127.8, 43.5 × 36 size µm. **15.** Slide 351–352 mm 1, 15 × 127.5, size 39 × 35 µm. **16–17.** Cyst of *Parvodinium inconspicuum* (Lemmermann) Carty. **16.** Slide 351–352 mm 1, 5.5 × 129.6, size 28 µm. **17.** Slide 360–361 mm 1, 4.8 × 137.8, size 32 µm.

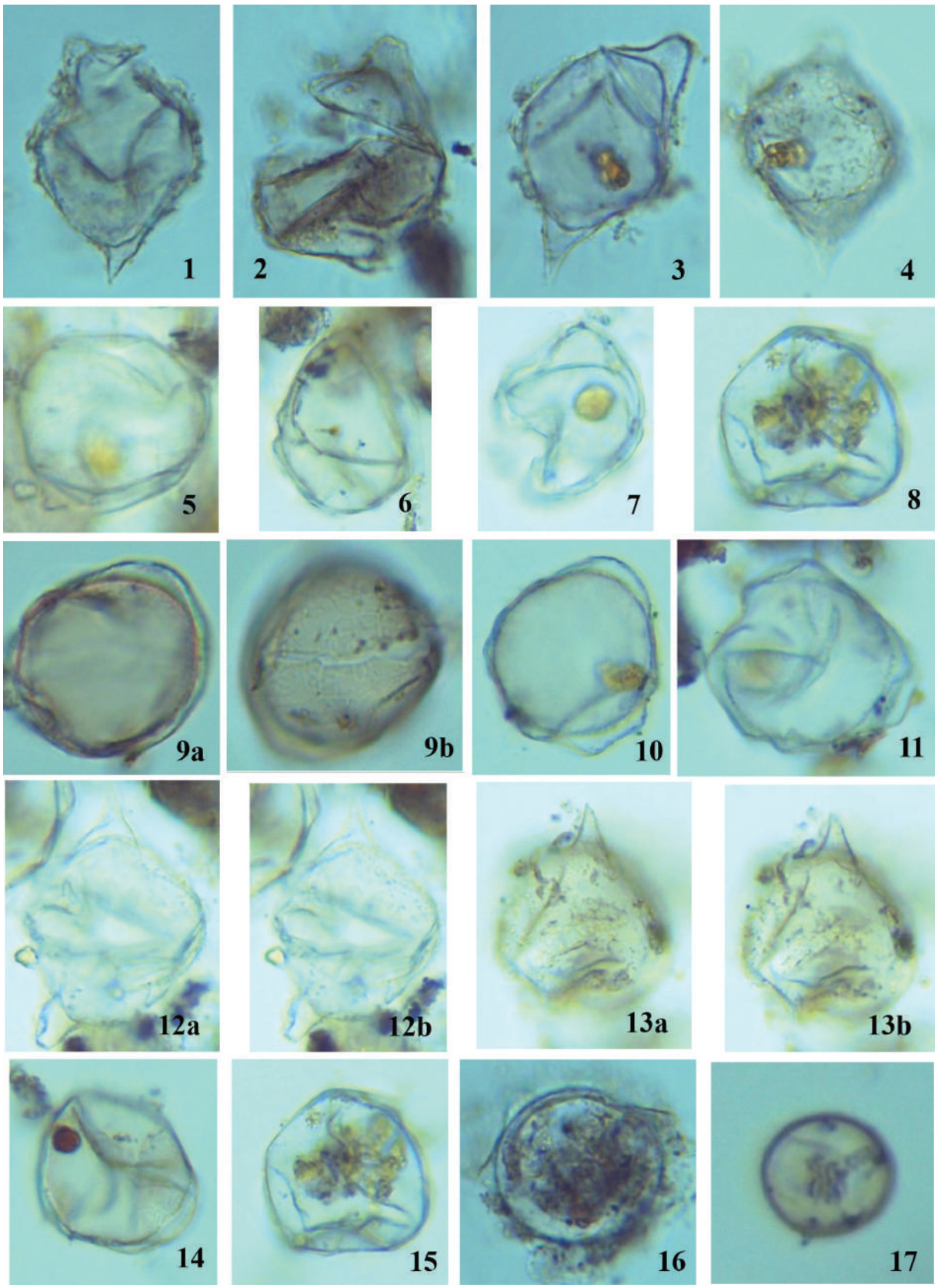

Figure 2

double-walled cysts, wall closely appressed and lacks ornamentation and sometimes with a barely visible sulcul indentation. Their red nuclei within the cyst indicate viable cell contents (McCarthy et al. 2013, 2017). According to Mertens et al. (2012) the archeopyle in the brown cysts of *Parvodinium inconspicuum* is hypocystal. Size range (based on eight specimens) 10–31 µm. Comments: Morphological description along with illustrations and previous occurrences of this species is discussed by Mertens et al. (2012). The thecae of *Parvodinium inconspicuum* are slightly larger (20–30 µm) with a distinct apical horn and scattered antapical spines (McCarthy & Kruger 2013).

1.6. Cyst of *Fusiperidinium wisconsinense* (Eddy) McCarthy et al. (Figure 2.1–4): These are proximate, cavate cysts slightly ellipsoidal in shape. They have a rounded, often bifurcated apical horn and a single, pointed antapical horn, both of almost equal length. The two wall layers are transparent, periphragm is ornamented by granules that are concentrated along parasutures, especially along the paracingulum. Both walls are appressed in the equatorial region. Archaeopyle, whenever observable, is epicystal/combination type composed of the apical plates 2′, 3′ and 4′ and part of the first apical plate (1′). The paraplates involved are often difficult to discern. Sometimes yellowish red cell content was observed within the cysts (McCarthy et al. 2011, 2017). Size range (based on 14 specimens) 30–41 × 39–58 µm. Comments: Morphological description along with illustrations and previous occurrences of this species is discussed by Mertens et al. (2012). McCarthy et al. (2018) proposed a new genus *Fusiperidinium* and transferred *Peridinium wisconsinense* to the newly proposed genus, instituting a new combination *Fusiperidinium wisconsinense*.

Several morphotypes appear to be dinoflagellate cysts, however, their identifications are tentative. They are as follows.

1.7. *Peridinium* sp. cf. ***P. bipes*** F. Stein (Figure 3.1–3): These are spherical, cavate cysts with thick and smooth walls (Mertens et al. 2012). The dinoflagellate cyst "Type C" in Norris & McAndrews (1970) was suggested to be a cyst of *Peridinium bipes*; with two walls, a periphragm and an endophragm. Size range (based on five specimens) 44–61 × 36–53 µm.

1.8. Dinoflagellate cyst type A (Figure 3.4): Size 89.5 × 111 µm.

1.9. Dinoflagellate cyst type B (Figure 3.5): Size 46.5 × 54 µm.

Figure 3. 1–3. Cyst of *Peridinium* sp. cf. *P. bipes* F. Stein. **1.** Slide 151–152 mm 2, 5.5 × 133.2, size 54.8 × 39 µm. **2.** Slide 160–161 mm 2, 9.8 × 128, size 49 × 36 µm. **3.** Slide 380–381 mm 1, 4.6 × 127.8, size 44 × 40 µm. **4.** Dinoflagellate cyst type A, slide 62–63 mm 1, 4.6 × 127.8, size 44 × 40 µm. **5.** Dinoflagellate cyst type B, slide 62–63 mm 2, 5 × 136.1, size 54 × 46.5 µm. **6.** Dinoflagellate cyst type C, slide 62–63 mm 2, 16 × 130.5, size 70.3 × 62.4 µm. **7.** Dinoflagellate cyst type D, slide 201–202 mm 1, 12 × 130, size 28.5 × 26 µm. **8.** Dinoflagellate cyst type E, slide 251–252 mm 1, 6 × 136, size 24.5 µm, horn 4 µm. **9.** Dinoflagellate cyst type F, slide 351–352 mm 1, 22 × 140, size 37 × 25 µm. **10.** Dinoflagellate cyst type G, slide 390–391 mm 1, 22 × 129, size 73 × 30 µm. **11.** *Pediastrum* type 1, slide 70–71 mm 1, 8 × 129.5, size 29 µm. **12.** *Pediastrum* type 2, slide 70–71 mm 1, 13.2 × 129, size 68.5 × 64 µm. **13.** *Spirogyra* zygospore, slide 9–10 mm 2, 13 × 138, size 25.5 × 19.5 µm. **14.** *Ovoidites* sp., slide 70–71 mm 1, 9.4 × 121.5, size 144 × 76 µm. **15.** *Spirogyra* zygospore, slide 140–142 mm 1, 11 × 126.2, size 112.5 × 43.5 µm. **16.** *Ovoidites* sp., slide 20–21 mm 1, 17 × 131.5, size 112.8 × 62.5 µm. **17.** *Botryococcus* sp., slide 20–21 mm 2, 16.3 × 132, size 24 × 16 µm. **18.** *Lecaniella* sp. (*Spirogyra* zygospore), slide 160–161 mm 1, 8.5 × 135.1 size 57.5 × 45.5 µm. **19.** Algal cell type 1, slide 50–51 mm 2, 22.3 × 142.3, size 46.8 × 48 µm. **20.** Algal cell type 2, slide 70–71 mm 1, 10.2 × 124.5, size 20.5 µm. **21.** Algal cell type 3, slide 101–102 mm 1, 4 × 140, size 17 µm. **22.** Algal cell type 4, slide 110–111 mm 1, 12.7 × 128.1, size 15 µm, spines 1–1.5 µm. **23.** Algal cell type 5, slide 190–191 mm 2, 6.2 × 133.2, size 20 µm. **24.** Algal cell type 6, slide 310–131 mm 2, 12 × 138, size 10 µm. **25.** Algal cell type 7, slide 340–341 mm 1, 6 × 133.9, size 35 × 20 µm. **26.** Algal cell type 8, slide 340–341 mm 1, 8.2 × 136.7, size 17.5 × 13.5 µm. **27.** Algal cell type 9, slide 370–371 mm 1, 3.5 × 131.8, size 32 × 23 µm. **28.** Algal cell type 10, slide 160–161 mm 1, 14.1 × 124.4, size 35 µm. **29.** Algal cell type 11, slide 160–161 mm 1, 22 × 130.5, size 42 µm. **30.** Algal cell type 12, slide 9–10 mm 2, 11.6 × 134.6, size 9.2 × 8.6 µm.

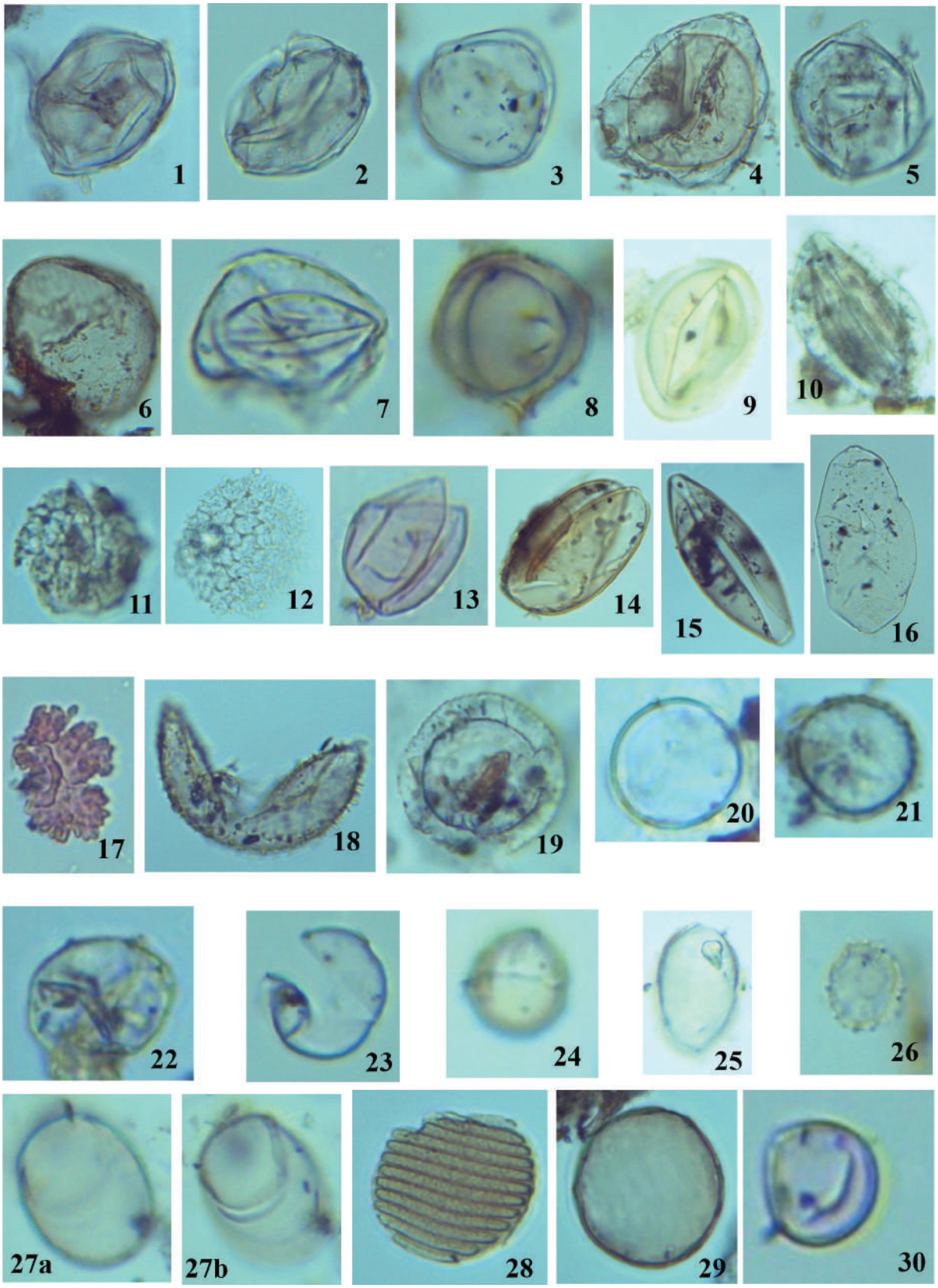
1
2
3
4
5
6
7
8
9
10
11
12
13
14
15
16
17
18
19
20
21
22
23
24
25
26
27a
27b
28
29
30

Figure 3

1.10. Dinoflagellate cyst type C (Figure 3.6): Size 46.5 × 54 µm. This morphotype looks like a cyst of freshwater dinoflagellate *Gonyaulax apiculata* (Kouli et al. 2001).

1.11. Dinoflagellate cyst type D (Figure 3.7): Size 28.5 × 26 µm

1.12. Dinoflagellate cyst type E (Figure 3.8): Size 24.5 µm, horn 4 µm

1.13. Dinoflagellate cyst type F (Figure 3.9): Size 37 × 25 µm

1.14. Dinoflagellate cyst type G (Figure 3.10): Size 73 × 30 µm

2. Algal Palynomorphs

The following algal morphotypes were observed.

2.1. *Pediastrum* type 1 (Figure 3.11): Size 29 µm.

2.2. *Pediastrum* type 2 (Figure 3.12): Size 68.5 × 64 µm.

2.3. *Spirogyra* zygospore (Figure 3.13): Size 25.5 × 19.5 µm.

2.4. *Ovoidites* sp. (Figure 3.14): Size 144 × 76 µm.

2.5. *Spirogyra* zygospore (Figure 3.15): Size 144 × 76 µm.

2.6. *Ovoidites* sp. (Figure 3.16): Size 112.8 × 62.5 µm.

2.7. *Botryococcus* sp. (Figure 3.17): Size 24 × 16 µm.

2.8. *Lecaniella* sp. (*Spirogyra* zygospore) (Figure 3.18): Size 57.5 × 45.5 µm.

2.9. Algal cell type 1 (Figure 3.19): Size 46.8 × 48 µm.

2.10. Algal cell type 2 (Figure 3.20): Size 20.5 µm.

2.11. Algal cell type 3 (Figure 3.21): Size 17 µm.

2.12. Algal cell type 4 (Figure 3.22): Size 15 µm, spines 1–1.5 µm.

2.13. Algal cell type 5 (Figure 3.23): Size 20 µm.

2.14. Algal cell type 6 (Figure 3.24): Size 10 µm.

2.15. Algal cell type 7 (Figure 3.25): Size 35 × 20 µm.

2.16. Algal cell type 8 (Figure 3.26): Size 17.5 × 13.5 µm.

2.17. Algal cell type 9 (Figure 3.27): Size 32 × 23 µm.

2.18. Algal cell type 10 (Figure 3.28): Size 35 µm.

Figure 4. 1. *Inapertisporites* type 1, slide 101–102 mm 2, 6 × 125.5, size 21.6 × 19.5 µm. **2.** *Inapertisporites* type 2, slide 201–202 mm 2, 19.5 × 123, size 36 µm. **3.** *Inapertisporites* type 3, slide 251–252 mm 2, 7 × 129.7, size 18.5 µm. **4.** *Inapertisporites* type 4, slide 251–252 mm 2, 6.4 × 138.3, size 41 × 27 µm. **5.** *Inapertisporites* type 5, slide 310–311 mm 2, 5 × 130, size 19.4 µm. **6.** *Palambages morulosa* (O. Wetzel 1961), slide 30–31 mm 1, 13.8 × 140.6, size 164 µm. **7.** *Multicellites* type 1, slide 40–41 mm 1, 9.5 × 132.3, size 23.5 × 7 µm. **8.** *Multicellite*s type 2, slide 70–71 mm 1, 6.5 × 132.7, size 53 × 16 µm. **9.** *Multicellite*s type 3, slide 101–102 mm 2, 2 × 123.5, size 19.2 × 13 µm. **10.** *Multicellite*s type 4, slide 360–361 mm 1, 15 × 124.1, size 43 × 13 µm. **11.** *Multicellite*s type 5, slide 251–252 mm 1, 22 × 138, 15 × 124.1 size 66 × 10.5 µm. **12.** *Multicellite*s type 6, slide 380–381 mm 1, 14 × 123.4, size 51 × 6.5 µm. **13.** *Dictyosporites* type 1, slide 50 × 51 mm 1, 2.8 × 139.5, size 34.5 × 30.7 µm. **14.** *Dictyosporites* type 2, slide 170–171 mm 1, 14.4 × 131.5, size 80.6 µm. **15.** *Dictyosporites* type 3, slide 251–252 mm 1, 13 × 127.7, size 19.6 µm. **16.** *Glomus* type 1, slide 101–102 mm 1, 8.6 × 137 size 62 × 65 µm, stalk length 122 µm. **17.** *Glomus* type 2, slide 50–51 mm 2, 5 × 133.8, size 44 × 35 µm. **18.** *Glomus* type 3, slide 50–51 mm 1, 13.2 × 130, size 34.3 × 27 µm. **19.** *Glomus* type 4, slide 201–202 mm 2, 6.5 × 129.2, size 21.6 µm. **20.** *Diporisporites* type 1, slide 51–52 mm 2, 9 × 134.2, size 51 × 27 µm. **21.** *Diporisporites* type 2, slide 70–71 mm 1, 4 × 130.2, size 11.4–14.2 × 8.8 µm. **22.** *Diporisporites* type 3, slide 151–152 mm 1, 21 × 127.8, size 21.6 × 14.6 µm. **23.** *Diporisporites* type 4, slide 210–211 mm 2, 4 × 145.7, size 27.5 × 18.5 µm. **24.** *Diporisporites* type 5, slide 310–311 mm 1, 9.5 × 133, size 21.5 × 12 µm. **25.** *Diporisporites* type 6, slide 380–381 mm 1, 3.5 × 133, size 61.5 × 5.5 µm. **26.** *Hypoxylonites* type 1, slide 62–63 mm 2, 3.5 × 133, size 41.8 × 21.5 µm. **27.** *Hypoxylonites* type 2, slide 140–141 mm 2, 5 × 127.5, size 163.4 × 33.5 µm. **28.** *Hypoxylonites* type 3, slide 70–71 mm 1, 19 × 130.5, size 38.7 × 14.5 µm. **29.** *Fractisporonites* sp., slide 110–111 mm 1, 17 × 124.5, size 75 × 4.5–6 µm. **30.** *Dicellaesporites* sp., slide 160–161 mm 1, 3.6 × 133.5, size 25, 22 µm.

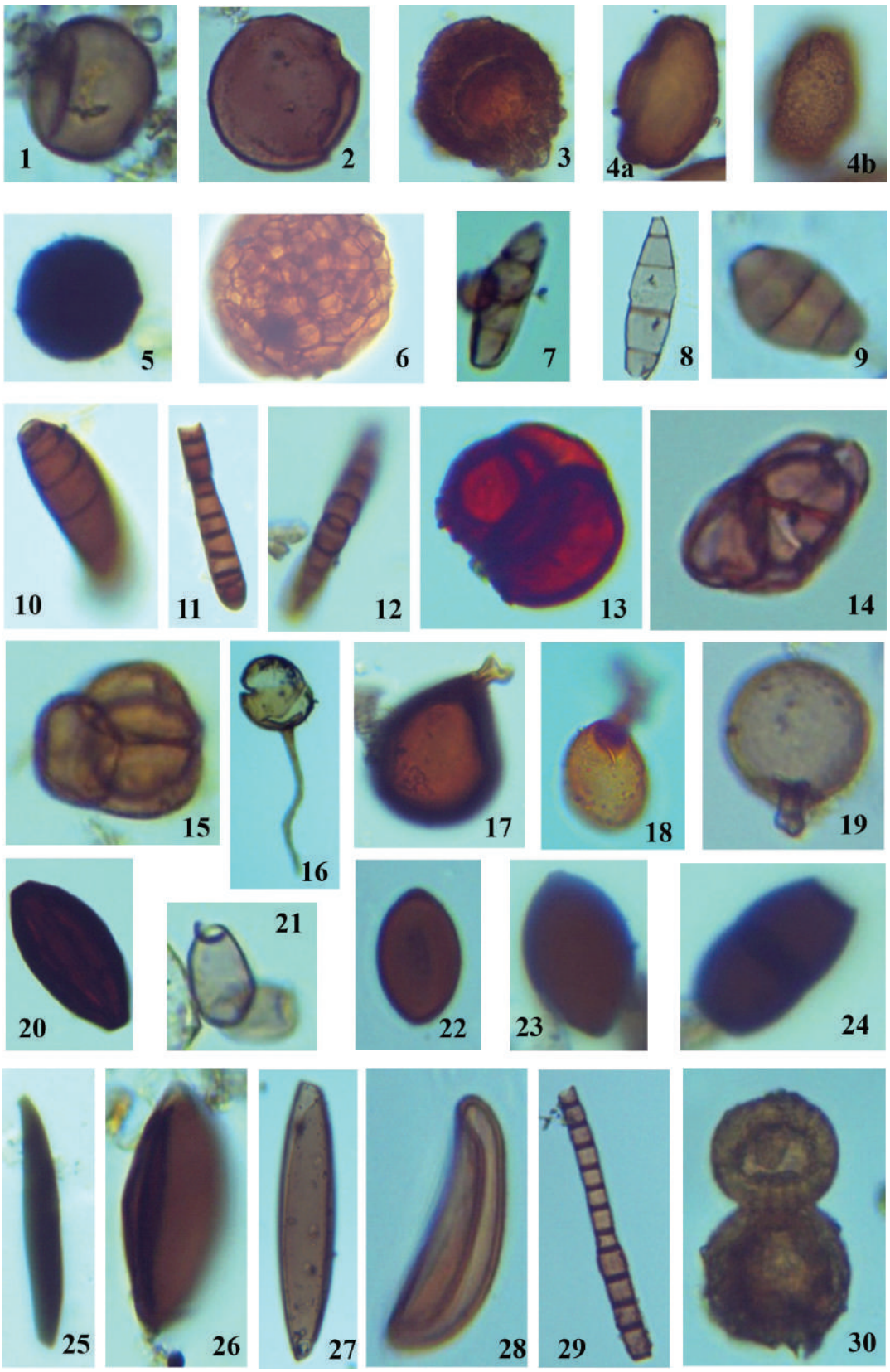
1
2
3
4a
4b
5
6
7
8
9
10
11
12
13
14
15
16
17
18
19
20
21
22
23
24
25
26
27
28
29
30

Figure 4

2.19. Algal cell type 11 (Figure 3.29): Size 42 µm; appears to be charophyte gyrogonite spheres. However, these forms are significantly smaller.

2.20. Algal cell type 12 (Figure 3.30): Size 9.2 × 8.6 µm; appears to be charophyte gyrogonite spheres. However, these forms are significantly smaller.

3. Fungal Spores and Hyphae

The following fungal morphotypes were observed.

3.1. *Inapertisporites* type 1 (Figure 4.1): Size 21.6 × 19.5 µm.

3.2. *Inapertisporites* type 2 (Figure 4.2): Size 36 µm.

3.3. *Inapertisporites* type 3 (Figure 4.3): Size 18.5 µm.

3.4. *Inapertisporites* type 4 (Figure 4.4): Size 41 × 27 µm.

3.5. *Inapertisporites* type 5 (Figure 4.5): Size 19.4 µm.

3.6. *Palambages morulosa* O. Wetzel 1961 (Figure 4.6): Size 164 µm.

3.7. *Multicellites* type 1 (Figure 4.7): Size 23.5 × 7 µm.

3.8. *Multicellites* type 2 (Figure 4.8): Size 23.5 × 7 µm.

3.9. *Multicellites* type 3 (Figure 4.9): Size 19.2 × 13 µm.

3.10. *Multicellites* type 4 (Figure 4.10): Size 43 × 13 µm.

3.11. *Multicellites* type 5 (Figure 4.11): Size 66 × 10.5 µm.

3.12. *Multicellites* type 6 (Figure 4.12): Size 51 × 6.5 µm.

3.13. *Dictyosporites* type 1 (Figure 4.13): Size 34.5 × 30.7 µm.

3.14. *Dictyosporites* type 2 (Figure 4.14): Size 80.6 µm.

3.15. *Dictyosporites* type 3 (Figure 4.15): Size 19.6 µm.

3.16. *Glomus* type 1 (Figure 4.16): Size 62 × 65 µm, stalk 122 µm.

3.17. *Glomus* type 2 (Figure 4.17): Size 44 × 35 µm.

3.18. *Glomus* type 3 (Figure 4.18): Size 34.3 × 27 µm.

3.19. *Glomus* type 4 (Figure 4.19): Size 21.6 µm.

3.20. *Diporisporites* type 1 (Figure 4.20): Size 51 × 27 µm.

3.21. *Diporisporites* type 2 (Figure 4.21): Size 11.4–14.2 × 8.8 µm.

Figure 5. 1. *Katora arabica* A. Kumar 2023, slide 390–391 mm 2, 12 × 123.1, size 75 × 62 µm, stalk length 14 µm. **2.** *Katora oblonga* A. Kumar 2023, slide 90–91 mm 1, 12 × 133.2, size 79.3 × 66 µm. **3.** *Katora oblonga* A. Kumar 2023, slide 220–221 mm 2, 6 × 128, size 96 × 73 µm. **4.** *Katora oblonga* A. Kumar 2023, slide 90–91 mm 1, 4.6 × 132.2, size 91 µm. **5.** *Katora oblonga* A. Kumar 2023, slide 160–161 mm 2, 18 × 129, size 84 µm. **6.** *Katora* type A, slide 210–211 mm 2, 17 × 149.5, size 94 × 91 µm. **7.** *Katora* type B, slide 360–361 mm 1, 13.7 × 123, size 150 × 78 µm. **8.** *Katora* type C, slide 351–352 mm 2, 4 × 128.5, size 28.5 × 22 µm, operculum 22 × 17 µm. **9.** *Palaeostomocystis fritilla*, slide 9–10 mm 2, 13 × 126.2, size 23.2 × 13 µm. **10.** *Palaeostomocystis fritilla*, slide 251–252 mm 2, 11.1 × 135.8, size 37 × 22.5 µm. **11.** Lorica of *Keratella* sp. slide 30–31 mm 2, 4.6 × 127.4, size 84 × 53 µm, spine length 31 µm and 15 µm. **12.** Rotifer lorica, slide 360–361 mm 1, 13 × 126.2, size 63 µm, mouth 31 µm. **13.** Chiromonid mandible, slide 50–51 mm 2, 20.2 × 124, size 125 × 52 µm. **14.** Chiromonid mandible, slide 201–202 mm 1, 20.2 × 124, size 69.5 × 26 µm. **15.** Chiromonid mandible, slide 210–211 mm 1, 5 × 145.5, size 52 × 38 µm. **16.** Chiromonid mandible, slide 330–331 mm 1, 13.2 × 134.5, size 135 × 45 µm. **17.** Cladoceran claw, slide 220–221 mm 2, 9 × 139.5, size 69.6 × 45 µm. **18.** *Bosmina longirostris* head capsule, slide 40–41 mm 2, 12.2 × 132.8, size 97.5 × 36 µm, appendage 116 × 17 µm. **19.** *Bosmina longirostris* head capsule, slide 62–63 mm 2, 9 × 134, size 138 × 131 µm, appendage 133 × 14 µm. **20.** *Daphnia pulex* (limb), slide 351–352 mm 1, 10 × 141.8, size 69 × 8 µm, dentitions 11–2.6 µm. **21.** *Eurycercus lamellatus* O.F. Muller (limb), slide 151–152 mm 2, 19.5 × 128, size 71 × 7.5 (longer limb), 27 × 2.4 µm (shorter limb). **22.** *Didymoporisporonites* type 1, slide 310–311 mm 1, 5 × 133.5, size 20 × 18.5 µm. **23.** *Didymoporisporonites* type 2, slide 320–321 mm 2, 12.5 × 137.7, size 78 × 62 µm, aperture 30.5 µm. **24.** *Papulosporonites* type 1, slide 340–341 mm 1, 6 × 133.8, size 46.5 × 35 µm. **25.** *Papulosporonites* type 2, slide 390–391 mm 1, 8.2 × 129.8, size 54 × 51.5 µm. **26.** *Monoporisporites* sp., slide 320–321 mm 1, 12 × 139.3, size 25 × 19 µm.

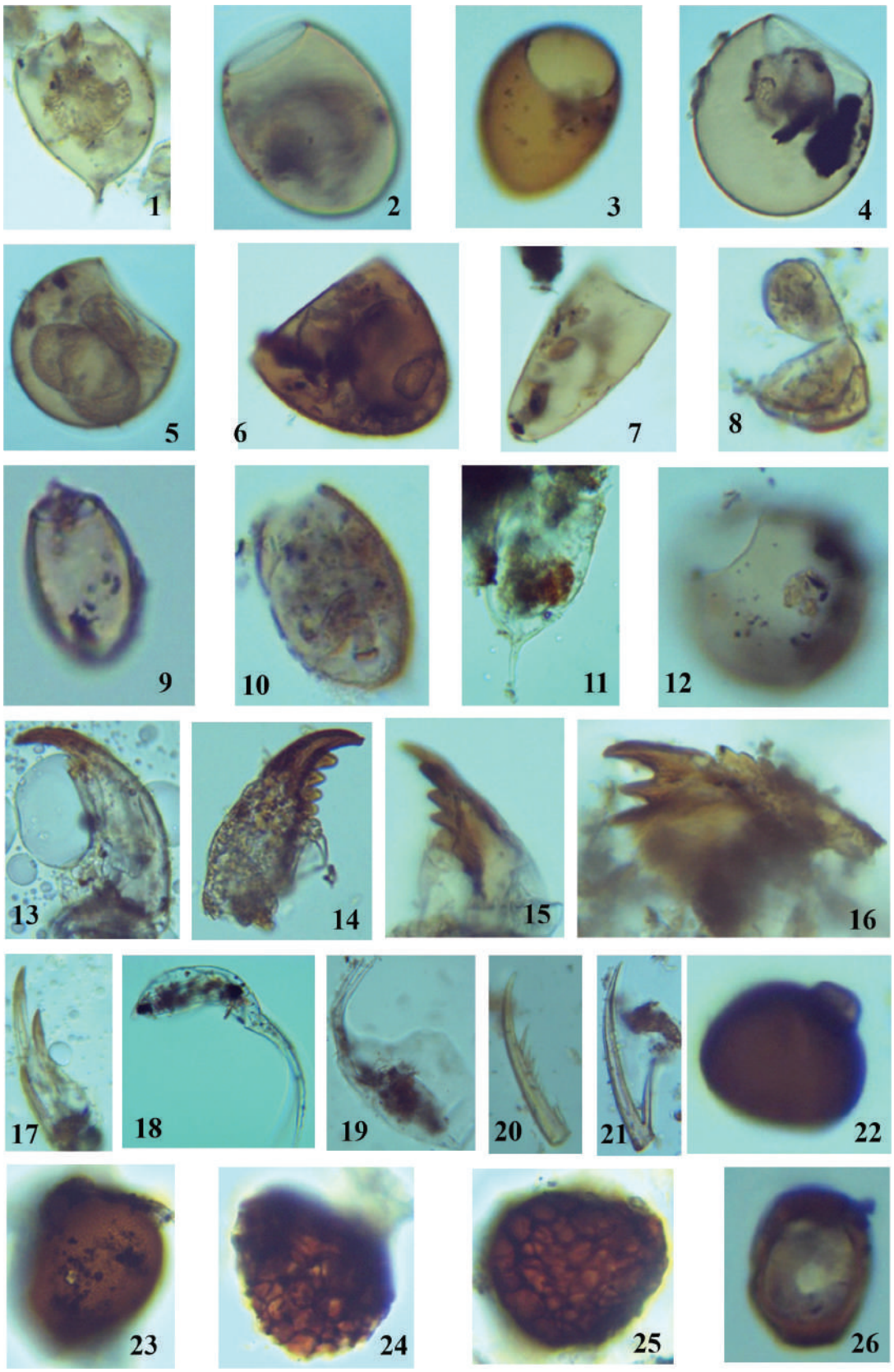

Figure 5

3.22. *Diporisporites* type 3 (Figure 4.22): Size 21.6 × 14.6 µm.

3.23. *Diporisporites* type 4 (Figure 4.23): Size 27.5 × 18.5 µm.

3.24. *Diporisporites* type 5 (Figure 4.24): Size 21.5 × 12 µm.

3.25. *Diporisporites* type 6 (Figure 4.25): Size 61.5 × 5.5 µm.

3.26. *Hypoxylonites* type 1 (Figure 4.26): Size 41.8 × 21.5 µm.

3.27. *Hypoxylonites* type 2 (Figure 4.27): Size 163.4 × 33.5 µm.

3.28. *Hypoxylonites* type 3 (Figure 4.28): Size 38.7 × 14.5 µm.

3.29. *Fractisporonites* sp. (Figure 4.29): Size 75 × 4.5–6 µm.

3.30. *Dicellaesporites* sp. (Figure 4.30): Size 25, 22 µm.

3.31. *Didymoporisporonites* type 1 (Figure 5.22): Size 20 × 18.5 µm.

3.32. *Didymoporisporonites* type 2 (Figure 5.23): Size 78 × 62 µm, aperture 30.5 µm.

3.33. *Papulosporonites* type 1 (Figure 5. 24): Size 46.5 × 35 µm.

3.34. *Papulosporonites* type 2 (Figure 5.25): Size 54 × 51.5 µm.

3.35. *Monoporisporites* sp. (Figure 5.26): Size 25 × 19 µm.

4. Zoomorphs

Several such morphotypes were observed and are described below.

4.1. *Katora arabica* A. Kumar 2023 (Figure 5.1): Size 75 × 62 µm, stalk length 14 µm. Similar morphotypes were described as Tintinnomorphs and Turbellarian egg capsules (Kumar 2023). McCarthy et al. (2021, Figure 5h) reported similar morphotype as egg capsule of flatworm *Gyratrix* sp.

4.2. *Katora oblonga* A. Kumar 2023 (Figure 5.2, 3): Size range (based on three specimens) 79.3–85 × 53.5–73 µm. This morphotype is oval, and similar morphotypes were described as Tintinnomorphs and Turbellarian egg capsules (Kumar 2023). Such morphotypes were also described as *Neorhabdocoela* (Class *Turbellaria*, Phylum *Platyhelmenthes*) egg capsule *Microdalyellia* type by Warner (1990, Figure 8-B), also as Neorhabdocoela oocyte type *Microdalyellia armigera* type 1-A from Early Holocene Lake "Wallisellen-Langachermoos" sediments in Switzerland by Hass (1996). Similarly, McCarthy et al. (2021) reported them as thick-walled resting eggs (oocytes) of flatworm *Microdalyellia* sp.

4.3. *Katora oblonga* A. Kumar 2023 (Figure 5.4, 5): Size range (based on eight specimens) 76.5–114 × 82–99 µm. This morphotype is spherical to subspherical, and similar morphotypes were described as Tintinnomorphs and Turbellarian egg capsules (Kumar 2023). Warner (1990) described a similar morphotype as spherical shaped egg capsule of *Neorhabdocoela* (Class: *Turbellaria*, Phylum: *Platyhelmenthes*). Similarly, Haas (1996) also reported them as Neorhabdocoela oocyte type *Strongylostoma radiatum* Type 1-A from Early Holocene Lake "Wallisellen-Langachermoos" sediments in Switzerland.

4.4. *Katora* type 1 (Figure 5.6): Cup-shaped, dark brown looks like type B of Mastuoka & Ando (2021) but without stalk. Size (one specimen) 94 × 91 µm, aperture 89 µm.

4.5. *Katora* type 2 (Figure 5.7): Elongated, sub triangular, gray. Size (one specimen) 150–78 µm, aperture 80 µm.

4.6. *Katora* type 3 (Figure 5.8): Subspherical, with attached operculum, gray, looks like morphotypes Figure 3: E and F in Mastuoka & Ando (2021). Size (one specimen) 28.5 × 22 µm, operculum 22 × 17 µm.

4.7. *Palaeostomocystis fritilla* Roncaglia 2004 (Figure 5.9, 10): Size range (based on two specimens) 37–23.2 × 22.5–13 µm. This form is like a fossilized ellipsoidal type of turbellarian

capsule (Matsuoka and Ando 2021). The genus *Palaeostomocystis* Deflandre 1937 has a debatable history about its biological affinity. Stover & Evitt (1978) considered it as dinoflagellate cyst, but Fensome et al. (2019) considered it an Acritarch. The Acritarch *Beringiella fritilla* (Bujak 1984) was transferred to *Palaeostomocystis* (Roncaglia 2004) thus instituting *Palaeostomocystis fritilla*. Comments: Morphotypes of modern and fossilized turbellarian egg capsules have very close morphological similarity with *Palaeostomocystis*, for example, the ellipsoidal type similar to *Gieystoria* sp. without a stalk is like the acritarch genus *Beringiella* or *Palaeostomocystis* (Matsuoka and Ando 2021). However, McCarthy et al. (2021) consider it as probable tintinnid often referred to as an acritarch. Most likely, the present specimens of *Palaeostomocystis fritilla* are turbellarian egg capsules, since turbellarians commonly inhabit lakes and tintinnids generally inhabit marine and brackish water environments. Hartman et al. (2018) reported the occurrence of *Palaeostomocystis* sp. cf. *P. fritilla* from a Holocene section offshore of Adélie Land (East Antarctica).

4.8. Lorica of *Keratella* sp. (Figure 5.11): Size 84 × 53 µm, spine length 31–15 µm.

4.9. Rotifer lorica (Figure 5.12): Size 63 µm, mouth 31 µm. This is a thin walled translucent morphotype.

4.10. Chiromonid mandibles (Figure 5.1, 13–16): Size range (based on four specimens) 135–52 × 45–26 µm. Chiromonids are also known as lake flies. Karima (2021) and McCarthy et al (2021) described such morphotypes as Chiromonid mandibles.

4.11. Cladoceran claw (Figure 5.17): Size 69.6 × 45 µm. Cladocera are mostly freshwater crustaceans, commonly known as water fleas are a diverse group of small crustaceans common in aquatic habitats.

4.12. *Bosmina longirostris* head capsule (Figure 5.18, 19): Size of specimen 18: 97.5 × 36 µm, appendage 116 × 17 µm. Size of specimen 19: 138 × 131 µm, appendage 133 × 14 µm. *Bosmina longirostris* is a species of water flea found in the Canadian Lakes.

4.13. *Daphnia pulex* (limb) (Figure 5.20): Size 69 × 8 µm, dentitions 11–2.6 µm (See Korhola & Rautio 2006, Figure 3, T).

4.14. *Eurycercus lamellatus* (limb) (Figure 5 21): Size 71 × 7.5 (longer limb), 27 × 2.4 µm (shorter limb) (See Korhola & Rautio 2006, Figure 3, U).

CONCLUSIONS

This palynological study is part of a broader palaeotempestology research project studying late Holocene sediments from lakes in the New Brunswick province of Atlantic Canada. The study is based on 40 lake gyttja samples from approximately 40 cm long core HV-CR from Harvey Lake in New Brunswick. The studied samples are approximately 10 mm apart. Generally, the samples yielded rich assemblages of well preserved and diverse groups of palynomorphs. A total of 300 palynomorphs were counted from each sample, excluding the fungal morphotypes. The counts included gymnosperm and angiosperm pollen; bryophytic and pteridophytic spores, algal palynomorphs, dinoflagellate cysts and zoomorphs. Gymnosperm and angiosperm pollen along with spores dominate the palynomorph assemblage (83.9%). Non-pollen palynomorphs (NPP) contribute only 16.81% of the assemblage that includes algal palynomorphs (4.27%), dinoflagellate cysts (7.6%), and zoomorphs (4.9%).

This study concentrates on studying cysts of freshwater dinoflagellates, following species were identified; *Peridinium gatunense* Nygaard, *Peridinium limbatum* (Stokes) Lemmermann, *Peridinium volzii* Lemmermann, *Peridinium willei* Huitfeldt-Kaas, *Parvodinium inconspicuum* (Lemmermann) Carty and *Fusiperidinium wisconsinense* (Eddy) McCarthy, Gu, Mertens &

Carbonell-Moore. In addition, rare specimens of *Peridinium* sp. cf. *P. bipes* and Dinoflagellate cyst types A, B, C, D, E, F and G were also observed. Several algal morphotypes such as *Pediastrum* types 1 and 2, Spirogyra zygospores, *Ovoidites* sp., *Botryococcu*s sp. and *Lecaniella* sp. (Spirogyra zygospore) were observed. Several unidentified algal cell types 1, 2, 3, 4, 5, 6, 7, 8, 9, 10, 11 and 12 are illustrated. The present assemblage of dinoflagellate cysts can be classified into group 1 of Danesh et al. (2024) which is an assemblage (primarily *Peridinium* spp.) associated with relatively shallow, mesotrophic lakes.

Several zoomorph morphotypes were observed. They are *Katora arabica* A. Kumar 2023; *Katora oblonga* A. Kumar 2023, *Katora* types 1, 2, and 3, *Palaeostomocystis fritilla* Roncaglia 2004; Lorica of *Keratella* sp., Rotifer lorica, Chiromonid mandibles, Cladoceran claw; *Bosmina longirostris* head capsule; *Daphnia pulex* (limb), and *Eurycercus lamellatus* (limb).

Although fungal palynomorphs were not counted in this study, several fungal morphotypes were observed and illustrated. They are as follows: *Inapertisporites* types 1, 2, 3, 4 and 5, *Palambages morulosa* O. Wetzel 1961, *Multicellites* types 1, 2, 3, 4, 5 and 6; *Dictyosporites* types 1, 2 and 3, *Glomus* types 1, 2, 3 and 4, *Diporisporites* types 1, 2, 3, 4, 5 and 6, *Hypoxylonites* types 1, 2 and 3, *Fractisporonites* sp., *Dicellaesporites* sp., *Didymoporisporonites* types 1 and 2, *Papulosporonites* types 1 and 2 and *Monoporisporites* sp.

This study extends the biogeographical distribution of freshwater dinoflagellate cysts to lakes in southern New Brunswick, Canada.

ACKNOWLEDGEMENTS

I thank Professor R.T. Patterson, Department of Earth Science, Carleton University, Ottawa for associating me in his research project on palaeotempestology study on late Holocene sediments of New Brunswick lakes in Canada and providing me with research material for this publication. I also thank Carling Walsh for maceration of the core samples and slide preparation for this study.

REFERENCES

Anderson T.W. 1985. Late-Quaternary pollen records from eastern Ontario, Quebec, and Atlantic Canada. In: Bryant Jr., V.M. & Holloway, R.G. (Editors) 1985. Pollen records of Late-Quaternary North American sediments. American Association of Stratigraphic Palynologists foundation, Dallas, Texas, 426 p.

Anderson T.W. 1988. Late Quaternary pollen stratigraphy of the Ottawa Valley – Lake Ontario region and its application in dating the Champlain Sea, pp. 195–206. In: Gadd N.R. (Editor) 1988. The Late Quaternary development of the Champlain Sea Basin. Geological Association of Canada, Special Paper 35. 312 p.

Battison L. & Brasier, M.D. 2012. Remarkably preserved prokaryote and eukaryote microfossils within 1 Ga-old lake phosphates of the Torridon Group, NW Scotland. Precambrian Research 196: 204–217, https://doi. org/10.1016/j.precamres.2011.12.012.

Bujak J.P. 1984. Cenozoic dinoflagellate cysts and acritarchs from the Bering Sea and northern North Pacific, D.S.D.P. Leg 19. Micropaleontology 30(2): 180–212.

Burden E.T., McAndrews J.H. & Norris G. 1986. Palynology of Indian and European forest clearance and farming in lake sediment cores from Awenda Provincial Park, Ontario. Canadian Journal of Earth Sciences 23: 43–54.

Chu G., Sun Q., Rioual P., Boltovskoy A., Liu Q., Sun P., Han J. & Liu J. 2008. Distinct microlaminations and freshwater ‘‘red tides’’ recorded in Lake Xiaolongwan, northeastern, China. Journal of Paleolimnology 39: 319–333.

Chu G., Sun Q., Wang X., Li D., Rioual P., Qiang L., Han J. & Liu J. 2009. A 1600-year multiproxy record of paleoclimatic change from varved sediments in Lake Xiaolongwan, northeastern China. Journal of Geophysical Research 114, D22108. doi:10. 1029/2009JD012077.

Clarke R.T. 1965. Fungal spores from Vermejo Formation coal beds (Upper Cretaceous) of Central Colorado. Mountain Geologist 2: 85–93.

Cook E.J. 2009. A record of late quaternary environments at lunette-lakes Bolac and Turangmoroke, Western Victoria, Australia, based on pollen and a range of non-pollen palynomorphs. Review of Palaeobotany and Palynology. 153(3–4): 185–224.

Cronin T.M. 1988. Paleozoogeography of postglacial Ostracoda from northeastern North America. Pp. 125–144. In: Gadd N.R. (Editor) 1988. The Late Quaternary development of the Champlain Sea Basin. Geological Association of Canada, Special Paper 35. 312 p.

Danesh D.C., McCarthy F.M.G., Volik O. & Drljepan M. 2013. Non-pollen palynomorphs as indicators of water quality in Lake Simcoe, Ontario, Canada. Palynology 37: 231–245.

Danesh D.C., McCarthy F.M.G., Sangiorgi F. & Cumming B.F. 2024.The utility of freshwater dinoflagellate cyst assemblages as a paleoecological proxy: An assessment from boreal lakes (northwest Ontario, Canada). Review of Palaeobotany and

Palynology 326 (2024) 105–128. https://doi.org/10.1016/j.revpalbo.2024.105128

Drljepan M., McCarthy F.M.G. & Hubeny J.B. 2014. Natural and cultural eutrophication of Sluice Pond, Massachusetts, USA, recorded by algal and protozoan microfossils. Holocene 24: 1731–1742.

Eddy S. 1930. The fresh-water armored or thecate dinoflagellates. Transactions of the American Microscopical Society 49: 277–321.

Elsik W.C. 1968. Palynology of a Palaeocene Rockdale lignite, Milam County, Texas. 1. Morphology and taxonomy. Pollen Spores 10(2): 263–314.

Elsik W.C. 1990. *Hypoxylonites* and *Spirotremesporites* form genera for Eocene to Pleistocene fungal spores bearing a single furrow. Palaeontographica Abt. B 216(1–6): 137–169.

Evitt W.R. & Wall D. 1968. Dinoflagellate studies IV. Theca and cyst of Recent freshwater *Peridinium limbatum* (Stokes) Lemmerman, Palo Alto (CA): Stanford University Publications. Geological Sciences. 12: 15p.

Félix J. 1894. Studienüber fossile Pilze; Zeitschrift der Deutschen Geologischen Gesellschaft 46: 269–280.

Fensome R.A., Taylor F.J.R. Norris G., Sarjeant W.A.S., Wharton D.I. & Williams G.L. 1993. A classification of fossil and living dinoflagellates. Micropaleontology Press Special Paper, no.7, 351 p.

Gelorini V., Verbeken A., van Geel B., Cocquyt C. & Verschuren D. 2011. Modern non-pollen palynomorphs from East African lake sediments. Review of Palaeobotany and Palynology 164: 143–173.

Harrington C.R. 1988. Marine mammals of the Champlain Sea, and the problem of whales in Michigan, pp. 225–240. In: Gadd N.R. (Editor) 1988. The Late Quaternary development of the Champlain Sea Basin. Geological Association of Canada, Special Paper 35. 312 p.

Hartman J.D., Bijl P.K. & Sangiorgi F. 2018. A review of the ecological affinities of marine organic microfossils from a Holocene record offshore of Ad´elie Land (East Antarctica). Journal of Micropalaeontology 37 (2): 445–497.

Haas J.N. 1996. Neorhabdocoela oocytes — palaeoecological indicators found in pollen preparations from Holocene freshwater lake sediments. Review of Palaeobotany and Palynology 91: 371–382.

Hunt A.S. & Rathburn A.E. 1988. Microfaunal assemblages of southern Champlain Sea piston cores. pp. 145–154. In: Gadd N.R. (Editor) 1988. The Late Quaternary development of the Champlain Sea Basin. Geological Association of Canada, Special Paper 35. 312 p.

Kalgutkar R.M. & Jansonius J. 2000. Synopsis of fungal spores, mycelia and fructifications. A.A.S.P. Contribution Series 39: 1–423.

Karima Z. 2021. Chironomidae: Biology, Ecology and Systematics. In: Perveen, F. K. (Ed) The wonders of *Diptera* – characteristics, diversity, and significance for the world's ecosystems. (pp. 1–25) DOI: 10.5772/intechopen.95577

Korhola A. & Rautio M. 2006. Cladocera and Other Branchiopod Crustaceans. In: Smol J.P., Birks H.J.B. & Last W.M. (Editors) 2001. Tracking Environmental Change Using Lake Sediments. Volume 4: Zoological Indicators. Kluwer Academic Publishers, Dordrecht, The Netherlands. (pp. 4–41) DOI: 10.1007/0-306-47671-1_2

Kouli K., Brinkhuis H. & Dale, B. 2001. *Spiniferites cruciformis*: a freshwater dinoflagellate cyst? Review of Palaeobotany and Palynology, 113 (4): 273–286. https://doi.org/10.1016/S0034-6667(00)00064-6

Krueger A.M. & McCarthy F.M.G. 2016. Great Canadian Lagerstätten 5: Crawford Lake – a Holocene lacustrine Konservat-Lagerstätte with two-century-old viable dinoflagellate cysts. Geoscience Canada, 43: 123–132, https://doi.org/10.12789/geocanj.2016.43. 086.

Kumar A. 2020. Palynology of the recent intertidal sediments of the Southern Red Sea Coast of Saudi Arabia. Palynology 45(1): 143–163. https://doi.org/10.1080/01916122.2020.1767708

Kumar A. 2023. New form taxa of non-pollen palynomorphs (NPP) from southern Red Sea coastal sediments of Saudi Arabia. Geophytology 53(1): 1–24.

Limaye R.B., Kumaran K.P.N., Nair K.M. & Padamlal D. 2007. Non-pollen palynomorphs as potential palaeoenvironmental indicators in the Late Quaternary sediments of the southwest coast of India. Current Science. 92(10): 1370–1382.

Limaye R.B., Padmalal D. & Kumaran K. 2017. Cyanobacteria and testate amoeba as potential proxies for Holocene hydrological changes and climate variability: evidence from tropical coastal lowlands of SW India. Quaternary International 443: 99–114.

Matsuoka K. & Ando T. 2021. Review: Turbellarian egg capsule as one type of aquatic palynomorph; reconsideration of Tintinnomorph. Laguna 28: 15–35.

McAllister D.E., Harrington C.R., Cumbaa S.L. & Renaud C.B. 1988. Paleoenvironmental and biogeographic analyses of fossil fishes in peri-Champlain Sea deposits in eastern Canada, pp. 242–258. In: Gadd N.R. (Editor) 1988. The Late Quaternary development of the Champlain Sea Basin. Geological Association of Canada, Special Paper 35. 312 p.

McCarthy F.M.G., Mertens K.N., Ellegaard M., Sherman K., Pospelova V., Ribeiro S., Blasco S. & Vercauteren D. 2011. Resting cysts of freshwater dinoflagellates in southeastern Georgian Bay (Lake Huron) as proxies of cultural eutrophication. Review of Palaeobotany and Palynology. 166(1–2): 46–62.

McCarthy F.M.G. & Kruger A.M. 2013. Freshwater dinoflagellates in palaeolimnological studies: *Peridinium* cysts as proxies of cultural eutrophication in the SE Great Lakes region of Ontario, Canada. In: Lewis J.M., Marret F. & Bradley L. (Editors) 2013. Biological and Geological Perspectives of Dinoflagellates. The Micropalaeontological Society, Special Publications. Geological Society, London, 133–139. http://www.geolsoc.org.uk/pub_ethic

McCarthy F.M.G., Drljepan M., Hubeny J.B., Krueger A.M., Pilkington P.M., Riddick N.L. & MacKinnon M.D. 2017. The influence of dissolved oxygen on dinoflagellate cyst distribution across Sluice Pond, a meromictic lake in NE Massachusetts, USA. Palynology, 41: 516–532. https://doi.org/10.1080/01916122. 2016.1276027

McCarthy F.M.G., Gu H., Mertens K.N., Carbonell-Moore C., Krueger A.M., Takano Y. & Matsuoka, K. 2018a. Transferring the freshwater dinoflagellate *Peridinium wisconsinense* (*Dinophyceae*) to the family *Thoracosphaeraceae*, with the description of *Fusiperidinium* gen. nov. Phycological Research 2018, 1–12. doi: 10.1111/pre.12215

McCarthy F.M.G., Riddick L., Volik O., Danesh D.C. & Krueger

A.M. 2018b. Algal palynomorphs as proxies of human impact on freshwater resources in the Great Lakes Region. Anthropocene, 21, 16–31, https://doi.org/10.1016/j.ancene.2017.11.004

McCarthy F.M.G., Pilkington P.M., Volik O., Autumn Heyde A. & Cocker S.L. 2021. Non-pollen palynomorphs in freshwater sediments and their palaeolimnological potential and selected applications. In: Marret F., O'Keefe J., Osterloff P., Pound M. & Shumilovskikh L. (Editors) 2021. Applications of non-pollen palynomorphs from palaeoenvironmental reconstructions to biostratigraphy. Geological Society, London, Special Publications 511: 121–150. https://doi.org/10.1144/SP511-2020-109

Mertens K.N., Rengefors K., Moestrup Ø. & Ellegaard M. 2012. A review of recent freshwater dinoflagellate cysts: taxonomy, phylogeny, ecology and palaeocology. Phycologia 51(6): 612–619.

Meyers P.A. & Ishiwatari R. 1993. Lacustrine organic geochemistry-an overview of indicators of organic matter sources and diagenesis in lake sediments. Org Geochem. 20: 867–900.

Montoya E., Rull V. & van Geel B. 2010. Non-pollen palynomorphs from surface sediments along an altitudinal transect of the Venezuelan Andes. Palaeogeogr. Palaeoclimatol. Palaeoecol. 297: 169–183.

Mott R.J. & Farley-Gill L.D. 1981. Two Late-Quaternary Pollen Profiles from Gatineau Park, Quebec. Geological Survey of Canada, Paper 80-31. 10 p.

Norris G. & McAndrews J.H. 1970. Dinoflagellate cysts from post-glacial lake muds, Minnesota (U.S.A.). Review of Palaeobotany and Palynology 10: 131–156.

Patterson R.T., Nasser N.A., Reinhardt E.G., Patterson C.W., Gregory B.R.B., Mazzella, V., Roe H.M. & Galloway J.M. 2022). End-member mixing analysis as a tool for the detection of major storms in lake sediment records. Paleoceanography and Paleoclimatology, 37, e2022PA004510. https://doi.org/10.1029/2022PA004510

Penaud A., Hardy W., Lambert C., Marret F., Masure E., Servais T., Siano R., Wary M. & Mertens K.N. 2018. Dinoflagellate fossils: Geological and biological applications. Revue de Micropaléontologie, 61 (3–4): 235–254. https://doi.org/10.1016/j.revmic.2018.09.003

Pfiester L.A. & Skvarla J.J. 1979. Heterothallism and thecal development in the sexual life history of *Peridinium volzii* (*Dinophyceae*). Phycologia 18: 13–18.

Rodrigues C.G. 1988. Late Quaternary invertebrate faunal associations and chronology of the western Champlain Sea basin. Pp. 155–176. In: Gadd N.R. (Editor) 1988. The Late Quaternary development of the Champlain Sea Basin. Geological Association of Canada, Special Paper 35, 312 p.

Roncaglia L. 2004. New acritarch species from Holocene sediments in central West Greenland, Grana, 43, 81–88, https://doi.org/10.1080/00173130410018966, 2004

Schmiedeknecht M. & Schwab G. 1964. Bulbillen fossiler Pilze aus einer tertiären Weichbraunkohle. Deutsche Akademie der Wissenschaften zu Berlin 6: 683–692.

Sheffy M.V. & Dilcher D.L. 1971. Morphology and taxonomy of fungal spores. Palaeontographica Abteilung B 133(1–3): 34–51.

Stover L.E. & Evitt W.R. 1978. Analyses of pre-Pleistocene organicwalled dinoflagellates. Stanford University Publications, Geological Sciences 15: 1–300.

Tardio M., Sangiorgi F., Brinkhuis H., Fillipi M.L., Cantonati M. & Lotter A.F. 2006. Peridinioid dinoflagellate cysts in a Holocene high-mountain lake deposits in Italy. Journal of Paleolimnology 36: 315–318.

Tardio M., Ellegaard M., Lundholm N., Sangiorigi F. & Di Giuseppe D. 2009. A hypocystal archeopyle in a freshwater dinoflagellate from the *Peridinium umbonatum* group (*Dinophyceae*) from Lake Nero di Cornisello, South-East Alps, Italy. European Journal of Phycology 44: 1–10.

Traverse A. 1955, Pollen analysis of the Brandon Lignite of Vermont, U.S. Bur. Mines Rept. of Investigations 5151.

Traverse A. 1994. Sedimentation of palynomorphs and palynodebris: an introduction. In Traverse, A. (Editor) Sedimentation of organic particles, Cambridge University Press 1–8.

Tulasne L.-R. & Tulasne C. 1845. Fungi nonullihypogaei, novi v. minus cogniti. Giornale Botanico Italiano 12(7–8): 55–63.

Van der Hammen T. 1954. El desarrollo de la flora Colombiana en los periodos geologicos–1. Maestrichtiano hasta Terciaro mas inferior (Una investigacion Palinologica de la formacion de Guaduas y equivalentes). Boletin Geologico (Bogota) 2(1): 49–106.

van Geel B. 1972. Palynology of a section from the raised peat bog "Wietmarscher Moor" with special reference to fungal remains. Acta Botanica Neerlandica 21(3): 261–284.

van Geel B. 1976. Fossil spores of *Zygnemataceae* in ditches of a pre-historic settlement in Hoogkarspel (The Netherlands). Review of Palaeobotany and Palynology. 22(4): 337–344.

van Geel B. 1986. Application of fungal and algal remains and other microfossils in palynological analyses. In: Bergland BE, editor. Handbook of Holocene palaeoecology and palaeohydrology. New York: Wiley; p. 497–505.

van Geel B. 2001. Non-pollen palynomorphs. In Smol JP, Birks HJB, Last W M (Editors) Tracking environmental change using lake sediments. v 3: terrestrial, algal, and siliceous indicators 99–119. Kluwer Academic Publishers, Dordrecht, The Netherlands.

Volik, O., McCarthy, F.M.G. & Riddick, N.L. 216. Insights from pollen, non-pollen palynomorphs and testate amoebae into the evolution of Lake Simcoe. Journal of Paleolimnology 56: 137–152 (2016). https://doi.org/10.1007/s10933-016-9900-8

Wall D. & Dale B. 1968. Modern dinoflagellate cysts and evolution of *Peridiniales*. Micropaleontology 14: 265–304.

Warner B.G. 1990. Methods in quaternary ecology#10. Other fossils. Geoscience Canada. 16(4): 231–242.

Wassenaar L., Brand U. & Terasmae J. 1988. Geochemical and paleoecological investigations using invertebrate macrofossils of the late Quaternary Champlain Sea, Ontario and Quebac. pp. 195–206. In: Gadd N.R. (Editor) 1988. The Late Quaternary development of the Champlain Sea Basin. Geological Association of Canada, Special Paper 35. 312 p.

Wetzel O. 1961. New microfossils from Baltic Cretaceous flintstones. Micropaleontology, 7: 337–350.

Zippi P., Yung Y.-K., McAndrews J.A., Norris G. & Welbourn P. 1990. An investigation of the potential of zygnematacean zygospores, *Peridinium*, and *Pediastrum* as paleo-indicators of recent lake acidification. Environmental Research: 1990 Technology Transfer Conference (Toronto, Canada), Proceedings 1, pp. 393–396.